INFLUENCE OF RADIATIVE HEAT AND MASS TRANSFER MECHANISM IN SYSTEM WATER DROPLET – HIGH-TEMPERATURE GASES ON INTEGRAL CHARACTERISTICS OF LIQUID EVAPORATION

by

Dmitrii O. GLUSHKOV, Genii V. KUZNETSOV, and Pavel A. STRIZHAK[*]

National Research Tomsk Polytechnic University, Tomsk, Russia

Physical and mathematical (system of differential equations in private derivatives) models of heat and mass transfer were developed to investigate the evaporation processes of water droplets and emulsions on its base moving in high-temperature (more than 1000 K) gas flow. The model takes into account a conductive and radiative heat transfer in water droplet and also a convective, conductive, and radiative heat exchange with high-temperature gas area. Water vapors characteristic temperature and concentration in small wall-adjacent area and trace of the droplet, numerical values of evaporation velocities at different surface temperature, the characteristic time of complete droplet evaporation were determined. Experiments for confidence estimation of calculated integral characteristics of processes under investigation – mass liquid evaporation velocities were conducted with use of cross-correlation recording video equipment. Their satisfactory fit (deviations of experimental and theoretical velocities were less than 15%) was obtained. The influence of radiative heat and mass transfer mechanism on characteristics of endothermal phase transformations in a wide temperature variation range was established by comparison of obtained results of numerical simulation with known theoretical data for "diffusion" mechanisms of water droplets and other liquids evaporation in gas.

Key words: *evaporation, heat and mass transfer, high-temperature gases,*
            droplets, water, vapor

Introduction

Up to the moment evaporation models were developed [1-9] which are applicable as a rule in limited variation ranges of parameters characterizing the heat intensity. Experiments [10-14] showed that assumptions accepted at approach development [1-9] relate mostly to description of heat and mass transfer mechanisms dominant under one or other condition.

In particular, the model of single water droplet evaporation [1-3] is considered to be the most popular one. In its terms, it is supposed the condition that all the energy get to droplet is consumed fully to implement the endothermal phase transformation. Conditions on *liquid-gas* boundary are described by group of expressions of the form Nu = 2 + f(Re, Pr) [1-3] at that convective heat exchange. It is known [1, 2] that this approach allows describing sufficiently completely heat exchange processes of *cold* solid sphere washed by heated

---

gas flow or *hot* particle washed by *cold* gas. It is quite acceptable to use this assumption for calculation of droplet evaporation velocities under conditions of *diffusive* [3] (evaporation process is limited by diffusion) liquid vapors reflux from vaporization surface. Solution of heat and mass transfer adjoint problems, when empirical values of heat exchange coefficients α are not used, is seem as the most reasonable as to conditions of intensive [15] (*kinetic*) evaporation mode (evaporation velocity is determined by liquid surface temperature) in high-temperature (more than 1000 K) gas area.

Attempts were made [16-18] to solve heat and mass transfer problems under conditions of intensive vaporization in adjoint formulations. Movement of single, small group and polydisperse flow of water droplets with sizes from 0.1 mm to 5 mm through gases (combustion products) with temperature about 1100 K was simulated [16-18]. Comparison of integral droplet evaporation characteristics obtained by using models [16-18] with the findings of experiments conducted in close conditions [12-14] showed the addition necessity of statements [16-18] with more detail processes description of energy supply to vaporization surface. In particular, the radiative mechanism of heat and mass transfer in the liquid droplet at its evaporation in the gas area with temperature more than 1000 K and also radiative heat supply on *liquid-gas* boundary is one of the most significative one under conditions of high-temperatures.

The purpose of the present work is a numerical investigation of radiative heat and mass transfer mechanism in *water droplet – high-temperature gases* system influence on integral characteristics of liquid evaporation under high temperature conditions.

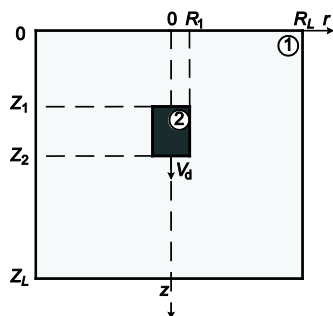## Heat and mass transfer model and methods of numerical investigations

Figure 1. Scheme of heat and mass transfer problem solution domain *1 – high-temperature gases, 2 – water droplet*

The problem was solved in a cylindrical system of coordinates (fig. 1) similar to formulations [16-18]. It was considered a droplet in form of a cylinder elongate toward moving. Droplet was moved through the gas area with temperature T_f, which exceeds significantly liquid temperature T_0. Droplet evaporation velocities, their existence time (*life* time) at intensive endothermal phase transformations implementations as well as temperatures and concentrations of gases and vapor in small droplet vicinity were calculated according to results of numerical simulation.

Radiative heat transfer in water droplet and radiant flux on *liquid-gas* boundary were taken into account additionally in opposite to models [16-18]. As a consequence the system of non-stationary non-linear differential equations describing the process under investigation appears as follows.

Energy equations for mixture of water vapors and high-temperature gases, and liquid droplet (with consideration for energy absorption of radiant heat flux):

$$C_1\rho_1 \frac{\partial T_1}{\partial t} = \lambda_1 \left(\frac{\partial T_1^2}{\partial r^2} + \frac{1}{r}\frac{\partial T_1}{\partial r} + \frac{\partial T_1^2}{\partial z^2} \right) \tag{1}$$

$$0 < r < R_L, \quad 0 < z < Z_1, \quad Z_2 < z < Z_L; \quad R_1 < r < R_L, \quad Z_1 < z < Z_2$$

$$C_2 \rho_2 \frac{\partial T_2}{\partial t} = \lambda_2 \left(\frac{\partial T_2^2}{\partial r^2} + \frac{1}{r} \frac{\partial T_2}{\partial r} + \frac{\partial T_2^2}{\partial z^2} \right) + \frac{\partial H(r)}{\partial r} + \frac{\partial H(z)}{\partial z} \tag{2}$$

$$0 < r < R_1, \quad Z_1 < z < Z_2$$

$$H(r) = H_{rd}\exp[-\chi(R_1 - r)], \quad 0 < r < R_1, \quad Z_1 < z < Z_2 \tag{3}$$

when
$$H_{rd} = \varepsilon\sigma(T_{3s}^4 - T_{2s}^4), \quad r = R_1, \quad Z_1 < z < Z$$

$$H(z) = H_{zd1}\exp[-\chi(z - Z_1)], \quad 0 < r < R_1, \quad Z_1 < z < Z_1 + 0.5(Z_2 - Z_1) \tag{4}$$

where
$$H_{zd1} = \varepsilon\sigma(T_{3s}^4 - T_{2s}^4), \quad z = Z_1, \quad 0 < r < R_1$$

$$H(z) = H_{zd2}\exp[-\chi(Z_2 - z)], \quad 0 < r < R_1, \quad Z_1 + 0.5(Z_2 - Z_1) \le z < Z_2 \tag{5}$$

where
$$H_{zd2} = \varepsilon\sigma(T_{3s}^4 - T_{2s}^4), \quad z = Z_2, \quad 0 < r < R_1$$

Equations of water vapor diffusion and balance of forming gas-vapor mixture:

$$\frac{\partial \gamma_w}{\partial t} = D_3 \left(\frac{\partial \gamma_w^2}{\partial r^2} + \frac{1}{r} \frac{\partial \gamma_w}{\partial r} + \frac{\partial \gamma_w^2}{\partial z^2} \right) \tag{6}$$

$$0 < r < R_L, \quad 0 < z < Z_1, \quad Z_2 < z < Z_L; \quad R_1 < r < R_L, \quad Z_1 < z < Z_2$$

$$\gamma_f + \gamma_w = 1, \quad 0 < r < R_L, \quad 0 < z < Z_1, \quad Z_2 < z < Z_L; \quad R_1 < r < R_L, \quad Z_1 < z < Z_2 \tag{7}$$

Boundary conditions are similar to statements [16-18]. Radiative heat transfer was taken into account additionally on *liquid-gas* bound opposite to models [16-18]:

$$T_1 = T_2, \quad \lambda_2 \frac{\partial T_2}{\partial r} = \lambda_1 \frac{\partial T_1}{\partial r} - Q_e W_e - \rho_3 C_3 V_e(T_{3s} - T_{2s}) + \varepsilon\sigma(T_{3s}^4 - T_{2s}^4) \tag{8}$$

at
$$r = R_1, \quad Z_1 < z < Z_2$$

$$T_1 = T_2, \quad \lambda_2 \frac{\partial T_2}{\partial z} = \lambda_1 \frac{\partial T_1}{\partial z} - Q_e W_e - \rho_3 C_3 V_e(T_{3s} - T_{2s}) + \varepsilon\sigma(T_{3s}^4 - T_{2s}^4) \tag{9}$$

at
$$z = Z_1, \quad z = Z_2, \quad 0 < r < R_1$$

Equation of droplet movement, methods, and algorithm of aerodynamic resistance coefficient c_χ computation as well as expressions used for calculation of liquid evaporation velocity W_e are similar to that one used at problem solving [16-18].

A system of non-stationary non-linear differential equations (1)-(9) in private derivatives was solved by the method of finite differences [19], the difference analogs of basic differential equations – by a local and 1-D method, non-linear equation – by iteration method. The sweep method [19] was used to solve the 1-D difference equations [19].

Adequate assessment of developed model and numerical simulation results was carried out with conservatism verification of used difference scheme, algorithms are similar to [20, 21], as well as comparison with experimental data (procedure and results are presented in the paper).

Numerical simulation results and their discussion

Numerical investigations of heat and mass transfer processes and phase transformations have been carried out for the next typical values: initial water droplet temperature T_0 = 300 K; gases temperature T_f = 1170 K; thermal effect of water evaporation Q_e = 2.26·10^6 J/kg; droplet dimensions R_d = (0.25-1)·10^{-3} m, Z_d = (1-4)·10^{-3} m; solution domain dimensions R_L = 0.1 m, Z_L = 1-5 m; initial droplet motion velocity V_0 = 0.5 m/s; molar mass of water M = 18 kg/kmol; dimensionless ratio of evaporation β = 0.1; aerodynamic resistance coefficient c_χ = 0.98; reduced power of droplet blackness ε = 0.85; water absorption coefficient χ = 0.7. Thermophysical characteristics of water, gases and water vapor were taken adequate [16-18].
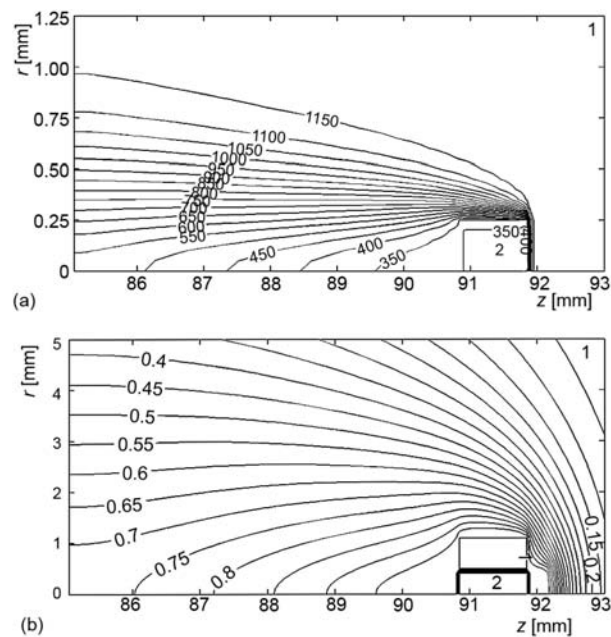
Figure 2 shows the typical isotherms and water vapor concentrations in small vicinity of droplet surface calculated according to models (1)-(9). It should be noted that presented isolines T and γ_w correspond sufficiently closely in general to similar arrangements which are in [16-18].

Numerical values of T and γ_w in the vicinity of the droplet as well as distance covered by it in high-temperature gas area are differ from [16-18]. In particular, temperature and concentrations of water droplets are more by 15-20% than that obtained with using models [16-18] under identical conditions. The motion resistance force increased due to more intensive vaporization. As a consequence distance covered by droplet in high-temperature gas area decreased by 7-12% in comparison with results [16-18].

Established effects can be explained by intensification of heat-up processes and, correspondingly, water evaporation in the concerned model due to radiative heat exchange. For example, fig. 3 shows temperature distributions in water droplet at different time moments. It is obvious that the process of droplet heat-up and its surface temperature increase is significantly non-linear.

Figure 2. (a) Isoterms *T* [K] and (b) concentrations of water vapors γ_w, for *t* = 0.1 s, R_d = 0.25 mm, and Z_d = 1 mm
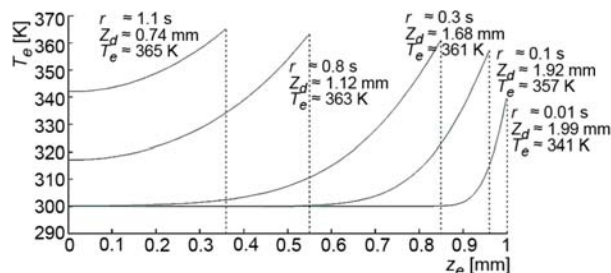

Figure 3. Temperature distributions in water droplet with initial values of R_d = 0.5 mm and Z_d = 2 mm at different time moments – on droplet symmetry axis (*R* = 0) when $Z_1 + 0.5(Z_2 - Z_1) < z < Z_2$

Glushkov, D., *et al.*, Influence on Radiative Heat and Mass Transfer Mechanism …
THERMAL SCIENCE, Year 2015, Vol. 19, No. 5, pp. 1541-1552

1545

Droplet surface temperature is sufficiently high (about 340 K) even at initial area ($t \leq 0.01$ s) of the water droplet motion trajectory. Droplet heat-up process is intensified (temperature in the droplet center increased up to 340 K, and on surface – up to 370 K) with growth of droplet motion (*staying*) time in high-temperature gas flow due to evaporation and consequently its sizes decrease. As a consequence, water evaporation velocity increases non-linearly under concerned conditions.

It was also established at the numerical simulation of the process under investigation that temperature gradients in water droplet near its forward, back and side surfaces (for concerned cylindrical form) are differed sufficiently significantly. Maximum values of this parameter are reached near the forward surface due to high gas temperature, fig. 2(b). Temperature of *washed* water vapors near side droplet surfaces are significantly lower than gas temperature at droplet front. As a consequence temperature gradient is significantly low in droplet and near its side surfaces than at its forward surface. Temperature of water vapors and gas mixture is far less, fig. 2(a) in trace of each droplet. Therefore the droplet temperature on its back surface differs incidentally from gas-vapor mixture temperature at this boundary.

One of the main investigation purposes was calculation of water evaporation mass velocities values under conditions of high-temperature heating. Results of W_e calculations at different surface temperatures are presented in fig. 4.

The established nature of influence presented in fig. 4, corresponds closely to the basic conclusions and deductions [15] and illustrates the *kinetic* mode of vaporization under concerned conditions of droplet and gas heat exchange. Also inference should be drawn that *diffusion* evaporation mode at gas temperature more than 1000 K is not implemented under any conditions.

Differences of temperature gradients at side, back, and end droplet evaporation surfaces, fig. 2(a) revealed at numerical simulation and dependence $W_e = f(T_e)$ (fig. 4) allow ex-

Figure 4. Evaporation velocity influence on droplet surface temperature

plaining the established significantly non-uniform change of droplet sizes relative to initial values of R_d and Z_d at evaporation. This leads to a non-linear change of complete droplet evaporation times too (this effect became still more observable with an allowance for radiative heat exchange in comparison with results [16-18]). Table 1 shows characteristic *life* (complete evaporation) times of water droplets with various sizes during its motion through gases with temperature 1170 K.
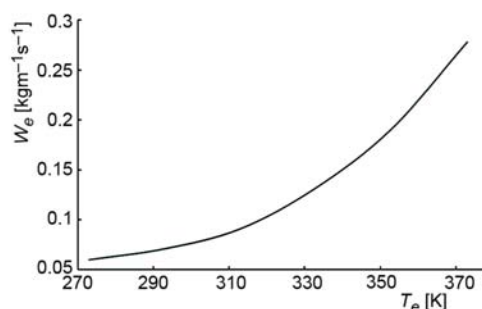
Table 1. Full evaporation time of water droplets with various initial sizes

R_d, [mm]	0.1	0.25	0.5	0.75	1
Z_d, [mm]	0.4	1	2	3	4
t_d, [s]	0.643	1.261	2.412	3.901	5.813

It is obvious from tab. 1 that values of droplet existence times differ from that obtained in [16-18] by 15-22%. At that difference of time t_d from similar parameters [16-18] de-

1546

Glushkov, D., *et al.*, Influence on Radiative Heat and Mass Transfer Mechanism …
THERMAL SCIENCE, Year 2015, Vol. 19, No. 5, pp. 1541-1552

creases with droplet size growth. This is due to defining the role of droplet boundary layers heat-up process. The difference of their heating dynamics in a model (1)-(9) and statements [16-18] at small (less than 0.5 mm) sizes is significant. Temperature differences at size growth for concerned heat transfer models in droplet reach 7-12 K. Temperature differences only on the droplet surface at their any sizes for model (1)-(9) and statements [16-18] is not less than 17-23 K. These results illustrate the considerable contribution of radiative heat exchange mechanism on *liquid-gas* boundary.

It should be noted that droplet evaporation velocity values (fig. 4) obtained as a result of theoretical investigations exceed significantly that one which obtained with using models [1-3]. Conditions of convective heat exchange on droplet surface is described with using expressions of the form Nu = 2 + f(Re, Pr) in accordance with approach [1-3]. Numerical estimations show that the values of W_e cannot exceed 0.05 kg/m^{2}s for conditions of conducted theoretical investigations in case of only convective heating. Physical features analysis of investigated processes allows drawing the inference that radiative heat exchange on droplet surface is definitive at high ($T_f > 1000$ K) gas temperatures. For example, convective and radiative flows for concerned conditions on the water droplet surface reach, accordingly:

$$q_c = \alpha(T_f - T_e) = 15(1100 - 370) \approx 10950 \text{ W/m}^2$$

$$q_l = \varepsilon\sigma(T_f^4 - T_e^4) = 0.95 \cdot 5.669 \cdot 10^{-8} \cdot (1100^4 - 370^4) \approx 77840 \text{ W/m}^2$$

It is visible that radiative heat flux from an external gas area exceeds the convective one more than in 7 times even at sufficiently large values of heat exchange coefficient α for conditions of conducted theoretical investigations (this correlation will be more than 10 at smaller α). It can be noted that the smaller diminution ($T_f - T_e$) is, the smaller difference is between flows q_c and q_l. But the condition $q_l > q_c$ is fulfilled even at gas temperature about 500 K. Therefore, most probably, it is sufficiently difficult to estimate the real values of W_e for *high-temperature gases – water droplets* system with using convective heating model [1-3]. Analysis shows that *convective* approximations can be used at gas temperatures not more than 500 K and commensurable flow values q_l and q_c.

A series of experiments were conducted to estimate the adequacy of the model (1)-(9) and possible *kinetic* mode implementation conditions of water droplet evaporation in high-temperature gas flow (fig. 1).

Procedure and result of experiments

Experimental methods and set-up (fig. 5) similar to present in [12-14] were used. Water droplets with predetermined initial sizes and velocities were emitted by dosing device and flew through the channel with high-temperature gases. Gas temperature corresponded to that one concerned above in heat and mass transfer problems (about 1150 K). Droplet evaporation velocities were determined with using optical methods of *tracer* visualization [22-24]. Sizes and mass of droplets at inlet into the high-temperature channel and at its outlet were recorded for that (fig. 5). As well as velocity values of droplet motion and liquid vapor outflow from their surface (in accordance with procedures [12-14] and algorithms [22-24]) were calculated.

Water droplets were emitted by dosing device with a frequency of 1 droplet per second in the carried out experiments. Additional experiments were carried out to stabilize the shape of emitted droplets. Two typical modes of change in shape of the droplet were studied during its moving through the high-temperature gases [12]. Besides, the reasons for implementation of such modes were established. Therefore, the parameters for the desired mode of

change in shape of the droplet and satisfactory repeatability of experimental results were selected due to varying the frequency of droplets emission, the tilt angle of the dosing device, the pressure before the dosing device. Not less than ten sets of experiments were carried out for each variant of initial conditions. Then, the results out of permissible limits were not to take into account. Analysis of systematic and random errors of measurement led to the conclusion about good repeatability of experimental results.

Basic characteristics of recording equipment (fig. 5): cross-correlation digital camera (3) with figure format 2048×2048 pixels, frame frequency not less than 1.5 Hz, minimal delay between two sequence figures not more than $5 \cdot 10^{-6}$ s; double pulsed solid-state laser (2) with wavelength length $532 \cdot 10^{-9}$ m, energy in impulse not less than $70 \cdot 10^{-3}$ J, impulse time not more than $12 \cdot 10^{-9}$ s, recurrence frequency not more than 15 Hz; synchronizing processor (5) with signal sampling not more than 10^{-8} s.

Figure 5. A scheme of experimental set-up
1 – laser emission generator, 2 – double pulsed solid-state laser, 3 – cross-correlation digital camera, 4 – personal computer, 5 – synchronizer of personal computer, cross-correlation digital camera and laser, 6 – light "pulse", 7 – vessel with liquid substance, 8 – channel of experimental liquid supply, 9 – dosing device, 10 – mount, 11 – experimental liquid droplets, 12 – cooling liquid channel of laser, 13 – cylinder from a heat-resistant translucent material, 14 – hollow cylinder with combustible liquid in internal medium, 15 – thermocouples, 16 – electronic weigher
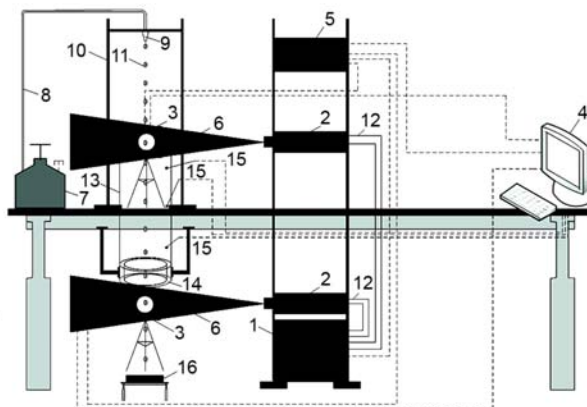
Titanium dioxide nanopowder particles (0.5% by weight) were added into water immediately before the experimentations to increase the videogram contract at laser illumination (similar to procedures [12-14]). The choice of TiO_2 powder as *tracers* is due to the fact that particles of this oxide do not dissolve in water and practically not influence on the vaporization process [12].

Droplet sizes in registration areas of videograms (before and after high-temperature gas area) were determined with using procedures [12-14] and optical method interferometric particle imaging (IPI) [26-28]. Droplets in registration area were illuminated many times (more than 10 times per second) by pulse (6). Droplet sizes in gas flow were calculated in a number of interference fringes observed on videograms. Condition radius R_d was chosen as a characteristic droplet size similar to experiments [12-14]. This is due to the fact that liquid droplets take ellipsoidal form (fig. 6) at the motion through gas area. Maximum diameters (from 6 to 10 values according to configuration) for these droplets were calculated and averaged. Average condition (droplet form is slightly different from sphere) radius R_d were calculated upon the obtained values.

Integral characteristics of droplet evaporation – changes of their sizes R_d and mass m_d in high-temperature gas area as well as time of motion through the channel (13) (t_m) were chosen as a function of experiment objective. Parameters ΔR, $\Delta R = [(R_d - R_d^*)/R_d]$ and Δm, $\Delta m = [(m_d - m_d^*)/m_d]$, where R_d^* and m_d^* are condition radius and mass of droplets at the outlet from the channel (13) were added under review. The maximum random errors of measurement for droplet sizes were 5%, for mass – 2%, and time – 4%. Errors of measuring and re-
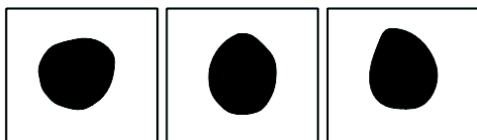
1548

Glushkov, D., *et al.*, Influence on Radiative Heat and Mass Transfer Mechanism …
THERMAL SCIENCE, Year 2015, Vol. 19, No. 5, pp. 1541-1552

Figure 6. Typical for conducted experiments images of water droplets moving through high-temperature gases (R_d = 2.5 mm)

cording devices for the droplet size determination did not exceed 1%, for mass – 2% and time – 1%, in accordance with procedures [12-14].

Exit velocities of *tracer* particles (correspond to water vapor outflow velocities into the gas area) from droplet surfaces were calculated with using optical method particle image velocimetry (PIV) [22-24] at the processing of videograms with droplet images. Flat of laser *light pulse* was considered to be the measuring area (fig. 5). *Tracer* particles in measuring area of flow (in a small vicinity of the droplet) were illuminated many times. Particle patterns were registered on digital cross-correlation video camera. The next processing of images allowed calculating the particle displacements in a time between flashes of light source (100 µs) and constructing the velocity fields of *tracers* [12-14]. Cross-correlation algorithm and fast Fourier transform method was used subject to conditions of correlation theorem [12-14]. Each videogram was divided in registry areas. After that cross-correlation function was calculated. The maximum of cross-correlation function corresponded to the most probable shift of particles in the registry area [12-14]. Momentary velocities of *tracers* were determined at a known time delays between laser flashes and the most probable particle movements (determined from the maximum of cross-correlation function) in registry areas of videoframes. Accuracy (method) errors of *tracer* velocity-finding device did not exceed 1% in accordance with procedures [12-14].

Results of videograms processing and liquid droplet mass measurement in series of experiments are in tab. 2.

Table 2. Characteristics of water droplet evaporation in high-temperature gas area

No. of experiment	R_d [mm]	R_d^* [mm]	$\rho_2 4\pi R_d^3/3$ [g]	$\rho_2 4\pi R_d^{*3}/3$ [g]	m_d [g]	m_d^* [g]	t_m [s]	W_e [kgm^{-2}s^{-1}] by eq. (11)
1	2.52	2.39	0.067	0.057	0.0667	0.0563	0.606	0.241
2	2.51	2.36	0.066	0.055	0.0656	0.0548	0.619	0.242
3	2.52	2.36	0.067	0.055	0.0673	0.0557	0.603	0.265
4	2.52	2.35	0.067	0.054	0.0674	0.0548	0.613	0.277
5	2.51	2.36	0.066	0.055	0.0668	0.0546	0.617	0.243

Values of mass water droplet evaporation velocity were established under concerned conditions at analysis of obtained parameters R_d, m_d, and t_m (tab. 2):

$$W_e = \frac{1}{S} \frac{dm}{dt} \qquad (10)$$

where $S = 4\pi R^2$ is the condition area of the droplet surface (R changes during droplet flight from R_d to R_d^*). Droplet mass is changed from m_d to m_d^*. It can be represented the condition droplet volume $V = 4\pi R^3/3$, and its condition mass $m = \rho_2 V$, where ρ_2 [kgm^{-3}] is the water density. In this case eq. (10) can be in the form:

$$W_e = \frac{\rho_2 (R_d - R_d^*)}{t_m} \qquad (11)$$

where derivative was changed by its difference analog $dR/dt \approx (R_d - R_d^*)/t_m$.

Glushkov, D., *et al.*, Influence on Radiative Heat and Mass Transfer Mechanism ...
THERMAL SCIENCE, Year 2015, Vol. 19, No. 5, pp. 1541-1552

1549

Calculated values of W_e (correspond satisfactorily to fig. 4) as well as droplet masses at the inlet and outlet from the channel are in tab. 2. Comparison of calculated droplet masses with measured ones in tab. 2 allows drawing the inference of legitimacy of condition droplet radius R_d usage as their characteristic size in concerned experiments. Good frequency of experimental results should be noted (tab. 2). Random errors of R_d and m_d determination did not exceed 1.5%.

It was established in experiments that values of *tracer* particle velocities in small (to 10 µm) *wall-adjacent* droplet area (obtained by PIV method [22-24]) are $V_v = 0.424$- -0.482 m/s. They correspond to velocities of liquid vapors outflow from droplet surfaces into gas area. Knowing the mass evaporation velocity W_e and velocity V_v of vapor outflow from evaporation surface estimated in experiments it can be determined the water vapor density in the immediate vicinity to this surface by expression $W_e = V_v \rho_3$. Processing of experiment results showed that values of ρ_3 are 0.568-0.573 kg/m³ under concerned conditions.

Constants of water droplet evaporation under concerned conditions can be determined at known values of W_e. Expression for liquid evaporation velocity is in the form [15]:

$$W_e = \frac{\beta}{1 - k_\beta \beta} \frac{P^n - P}{\sqrt{\dfrac{2\pi R_t T_e}{M}}} . \tag{12}$$

Results of numerical investigations presented show that droplet surface temperature (T_e) during their motion through high-temperature gases reach 365 ± 10 K, in other words it is equal to the maximum possible temperature of water evaporation. It can be accepted well founded that the water vapor temperature in the immediate vicinity of evaporation surface under conditions of intensive vaporization and, correspondingly, formation of droplets with thin *buffer* (vapory) layer is practically not differed from the temperature of phase interface $T_v \approx T_e$. Vukalovich-Novikov constitutive equation for overheated water vapor can be used to determine the pressure of gas-vapor area immediately near to *liquid-gas* boundary because gas concentrations are minimal, fig. 2(b) and relative volume fractions of *tracer* nanopowder particles TiO_2 are not exceed 1% in small *wall-adjacent* droplet area in consequence of *buffer* layer formation [25]:

$$\left(P + \frac{a}{\left(\dfrac{1}{\rho_3}\right)^2} \right) \left(\frac{1}{\rho_3} - b \right) = \frac{R_t T_e}{M} \left(1 - \frac{c'}{\dfrac{1}{\rho_3} T_e^{\frac{3+2m}{2}}} \right), \tag{13}$$

where $a = 620$ Nm⁴/kg², $b = 0.0009$ m³/kg, $R_t = 8.314$ L/molK, $M = 18$ kg/kmol, $c' = 405000$ m³K/kg, and $m = 1.968$ in accordance with [25].

It is obtained from eq. (13) with maximum possible temperature of the phase interface surface $T_e = 373$ K and $\rho_3 = 0.568$-0.573 kg/m³, that vapor pressures near the droplet surface are $(0.979$-$0.988)\cdot10^5$ N/m². As a consequence, $P^n - P \approx 2560$-3450 N/m². Expression $\beta/(1 - k_\beta \beta)$ is 0.0726-0.1121 at $P^n - P \approx 2560$-3450 N/m² and $T_e = 373$ K, it was obtained with using experimental values of evaporation velocities $W_e = 0.241$-0.277 kg/m²s and formulas (12). Parameter k_β value, as a rule, is accepted equal to 0.396-0.432 [15]. Then the range $\beta = 0.0703$-0.1072 can be marked for evaporation coefficient and it can be drawn the infer-

ence that established values of constant β correspond to maximum possible liquid evaporation velocities under concerned conditions (coefficient β was accepted equal to 0.1 at numerical solution similar to statements [16-18]).

Conducted series of experiments showed that W_e values are changed relatively to that one adduced in tab. 2 at variation of R_d and Z_d initial values in sufficiently wide ranges presented above. Nature of W_e change corresponds closely to fig. 4. So marked values of β and k_β can be used at simulation of heat and mass transfer processes in the vicinity of water droplets moving in high-temperature gas area at change of their characteristic sizes in sufficiently wide and typical for many supplements ranges, $R_d = (0.25\text{-}1)\cdot 10^{-3}$ m, $Z_d = (1\text{-}4)\cdot 10^{-3}$ m. Comparison of experimental investigation results and conducted theoretical analysis allows drawing the inference that *kinetic* [15] evaporation mode when evaporation velocity depends on liquid droplet surface temperature (fig. 4) is implemented under condition of high temperatures of outdoor environment.

The results of an experimental analysis of droplets size and weight change characteristics in moving in high-temperature gas flow are presented in publications [29-31]. The influence of environmental parameters, liquid droplet properties, their composition, sizes and velocities of motion has been analyzed. The characteristic regularities of drops braking in counter high-temperature flow, their reversal, coagulation, fragmentation, dispersion and collisions have been also studied [32-35]. A joint influence of neighboring drops on the conditions of their evaporation has been established. In general, the results obtained from numerical simulation in the present work correlate well with the experimental data [29-35].

Conclusions

- Radiative heat transfer at *liquid-gas* boundary under conditions of high temperatures in concerned system (fig. 1) is determinative. Radiative (q_l) heat flux exceeds the convective one (q_c) in several times. Heat transfer due to emission in the droplet is also intensified sufficiently the droplet heat-up and, correspondingly, water evaporation despite the relatively small temperature gradient inside it.
- Variation ranges of water evaporation velocities W_e established at numerical simulation and in experiments exceed significantly the values which can be obtained by using *diffusion* models [1-3]. First of all revealed effects is due to radiative energy transfer which is not taken into account in models of convective heat exchange [1-3].
- The results of numerical investigations are in good agreement with integral evaporation characteristics obtained in conducted experiments. A well-founded conclusion can be done about developed heat and mass transfer model adequacy. It can also be concluded that it is expedient to solve the adjoint heat and mass transfer problems under conditions of high-temperature liquid droplet evaporation to approximate the results of numerical investigations to real processes.

Nomenclature

C – constant specific heat, [$\text{Jkg}^{-1}\text{K}^{-1}$]

c_χ – dimensionless resistance coefficient, [–]

D – diffusion coefficient, [m^2s^{-1}]

g – gravitational acceleration, [ms^{-2}]

$H(r)$, $H(z)$ – radiant flow density in droplet, [Wm^{-2}]

H_{rd}, H_{zd1}, H_{zd2} – radiant flow densities on droplet surface, [Wm^{-2}]

k_β – dimensionless coefficient, [–]

M – painting mass of water, [kgkmol^{-1}]

m_d – droplet mass, [g]

Δm – relative difference of droplet mass at outlet and inlet into high-temperature channel in experiments, [g]

Nu – Nusselt number, [–]

P – pressure of water vapor near the phase transition border, [Nm^{-2}]

P^n – pressure of saturated water vapor, [Nm^{-2}]
Pr – Prandtl number, [–]
Q_e – thermal reaction coefficient of evaporation, [Jkg^{-1}]
q_c, q_l – convective and radiative flow on droplet surface, [Wm^{-2}]
R_d, Z_d – drop dimensions, [m]
R_L, Z_L – solution domain dimensions, [m]
R_t – universal gas constant (= 8.31), [$Jmol^{-1}K^{-1}$]
Re – Reynolds number, [–]
ΔR – relative difference of droplet sizes at outlet and inlet into the high-temperature channel in experiments, [g]
r, z – co-ordinates of the cylindrical system, [m]
T – temperature, [K]
T_0 – initial water temperature, [K]
T_e – evaporated droplet surface temperature, [K]
T_f – initial gas temperature, [K]
T_v – water vapor temperature near droplet surface, [K]
T_{2s}, T_{3s} – temperature of water and vapors in the vicinity of the phase transition border, [K]
t – time, [s]
t_d – time of full evaporation, [s]

t_m – time of droplet movement through the high-temperature channel, [s]
V – relative volume of droplet, [m^3]
V_d – droplet movement velocity, [ms^{-1}]
V_e – velocity of water vapors from the corresponding droplet surface, [ms^{-1}]
W_e – mass velocity of evaporation, [$kgm^{-2}s^{-1}$]

Greek symbols

α – heat-exchange coefficient, [$Wm^{-2}K^{-1}$]
β – dimensionless coefficient of condensation (evaporation), [–]
γ_f – dimensionless concentration of gases, [–]
γ_w – dimensionless concentration of water vapors, [–]
ε – reduced emissivity factor, [–]
λ – thermal conductivity, [$Wm^{-1}K^{-1}$]
ρ – density, [kgm^{-3}]
σ – Stefan-Boltzmann constant (= $5.67 \cdot 10^{-8}$), [$Wm^{-2}K^{-4}$]
χ – extinction coefficient, [–]

Subscripts

1 – high-temperature gases
2 – water droplet
3 – water vapors

Acknowledgments

References

[1] Ranz, W. E., Marshall, W. R., Evaporation from Drops – I, II, *Chemical Engineering Progress*, *48* (1952), pp. 141-146, pp. 173-180
[2] Fuchs, N. A., *Evaporation and Droplet Growth in Gaseous Media*, Pergamon Press, London, 1959
[3] Terekhov, V. I., *et al.*, Heat and Mass Transfer in Disperse and Porous Media Experimental and Numerical Investigations of Non-Stationary Evaporation of Liquid Droplets, *Journal of Engineering Physics and Thermophysics, 83* (2010), 5, pp. 883-890
[4] Sazhin, S. S., *et al.*, Models for Droplet Transient Heating: Effects on Droplet Evaporation, Ignition, and Break-up, *International Journal of Thermal Sciences, 44* (2005), 7, pp. 610-622
[5] Stefanović, P., *et al.*, Numerical Modeling of Disperse Material Evaporation in Axisymmetric Thermal Plasma Reactor, *Thermal Science, 7* (2003), 1, pp. 63-100
[6] Morales-Ruiz, S., *et al.*, Numerical Resolution of the Liquid-Vapour Two-Phase Flow by Means of the Two-Fluid Model and a Pressure Based Method, *Int. J. of Multiphase Flow, 43* (2012), July, pp. 118-130
[7] Fedorets, A. A., *et al.*, Coalescence of a Droplet Cluster Suspended over a Locally Heated Liquid Layer, *Interfacial Phenomena and Heat Transfer, 1* (2013), 1, pp. 51-62
[8] Shanthanu, S., *et al.*, Transient Evaporation of Moving Water Droplets in Steam – Hydrogen – Air Environment, *International Journal of Heat and Mass Transfer, 64* (2013), Sept., pp. 536-546
[9] Gatapova, E. Ya., *et al.*, Evaporation of a Sessile Water Drop on a Heated Surface with Controlled Wettability, *Colloids and Surfaces A: Physicochemical and Engineering Aspects, 441* (2014), Jan., pp. 776-785
[10] Zeng, Y., Lee, C. F., A Model for Multicomponent Spray Vaporization in a High-Pressure and High-Temperature Environment, *Journal of Engineering for Gas Turbines and Power, 124* (2002), 3, pp. 717-724
[11] Varaksin, A. Yu., Fluid Dynamics and Thermal Physics of Two-Phase Flows: Problems and Achievements, *High Temperature, 51* (2013), 3, pp. 377-407

1552

Glushkov, D., *et al.*, Influence on Radiative Heat and Mass Transfer Mechanism …
THERMAL SCIENCE, Year 2015, Vol. 19, No. 5, pp. 1541-1552

[12] Volkov, R. S., *et al.*, Experimental Study of the Change in the Mass of Water Droplets in Their Motion through High-Temperature Combustion Products, *Journal of Engineering Physics and Thermophysics, 86* (2013), 6, pp. 1413-1418

[13] Kuznetsov, G. V., Strizhak, P. A., The Motion of a Manifold of Finely Dispersed Liquid Droplets in the Counterflow of High-Temperature Gases, *Technical Physics Letters, 40* (2014), 6, pp. 519-522

[14] Volkov, R. S., *et al.*, Influence of the Initial Parameters of Spray Water on Its Motion through a Counter Flow of High Temperature Gases, *Technical Physics, 59* (2014), 7, pp. 959-967

[15] Avdeev, A. A., Zudin, A. A., Kinetic Analysis of Intensive Evaporation (Method of Reverse Balances), *High Temperature, 50* (2012), 4, pp. 527-535

[16] Vysokomornaya, O. V., *et al.*, Heat and Mass Transfer in the Process of Movement of Water Drops in a High-Temperature Gas Medium, *Journal of Eng. Phys. and Thermophys., 86* (2013), 1, pp. 62-68

[17] Kuznetsov, G. V., Strizhak, P. A., Numerical Investigation of the Influence of Convection in a Mixture of Combustion Products on the Integral Characteristics of the Evaporation of a Finely Atomized Water Drop, *Journal of Engineering Physics and Thermophysics, 87* (2014), 1, pp. 103-111

[18] Glushkov, D. O., *et al.*, Numerical Investigation of Water Droplets Shape Influence on Mathematical Modeling Results of Its Evaporation in Motion through a High-Temperature Gas, *Mathematical Problems in Engineering*, *2014* (2014), ID 920480

[19] Samarskii, A. A., *The Theory of Difference Schemes*, Marcel Dekker, USA, 2001

[20] Kuznetsov, G. V., Strizhak, P. A., On the Possibility of Using a One-Dimensional Model for Numerical Analysis of the Ignition of a Liquid Condensed Material by a Single Heated Particle, *Combustion, Explosion and Shock Waves, 46* (2010), 6, pp. 683-689

[21] Kuznetsov, G. V., Strizhak, P. A., Transient Heat and Mass Transfer at the Ignition of Vapor and Gas Mixture by a Moving Hot Particle, *Int. J. of Heat and Mass Transfer, 53* (2010), 5-6, pp. 923-930

[22] Raffel, M., *et al.*, *Particle Image Velocimetry*, Springer, Berlin, 1998

[23] Foucaut, J. M., Stanislas, M., Some Considerations on the Accuracy and Frequency Response of Some Derivative Filters Applied to Particle Image Velocimetry Vector Fields, *Measurement Science and Technology, 13* (2002), 7, pp. 1058-1071

[24] Damaschke, N., *et al.*, Optical Limits of Particle Concentration for Multi-Dimensional Particle Sizing Techniques in Fluid Mechanics, *Experiments in Fluids, 32* (2002), 2, pp. 143-152

[25] Baehr, H. D., Stephan, K., *Heat and Mass Transfer*, Springer Verlag, Berlin, 1998

[26] Glantschnig, W. J., Chen, S., Light Scattering from Water Droplets in the Geometrical Optics Approximation, *Applied Optics*, *20* (1981), 14, pp. 2499-2509

[27] Konig, G. *et al.*, A New Light-Scattering Technique to Measure the Diameter of Periodically Generated Moving Droplets, *J. of Aerosol Sci.*, *17* (1986), 2, pp. 157-167

[28] Kawaguchi, T. *et al.*, Size Measurements of Droplets and Bubbles by Advanced Interferometric Laser Imaging Technique, *Meas. Sci. and Technol.*, *13* (2002), 3, pp. 308-316

[29] Kuznetsov, G. V., Strizhak, P. A. Evaporation of Single Droplets and Dispersed Liquid Flow in Motion through High Temperature Combustion Products, *High Temperature, 52* (2014), 4, pp. 568-575

[30] Vysokomornaya, O. V., *et al.*, Experimental Investigation of Atomized Water Droplet Initial Parameters Influence on Evaporation Intensity in Flaming Combustion Zone, *Fire Safety J., 70* (2014), Nov., pp. 61-70

[31] Volkov, R. S., *et al.*, The influence of Initial Sizes and Velocities of Water Droplets on Transfer Characteristics at High-Temperature Gas Flow, *Int. J. of Heat and Mass Transfer, 79* (2014), Dec., pp. 838-845

[32] Volkov, R. S., *et al.*, Mechanism of Liquid Drop Deformation in Subsonic Motion in a Gaseous Medium, *Journal of Engineering Physics and Thermophysics, 87* (2014), 6, pp. 1351-1361

[33] Volkov, R. S., *et al.*, Analysis of the Effect Exerted by the Initial Temperature of Atomized Water on the Integral Characteristics of Its Evaporation during Motion through the Zone of "Hot" Gases, *Journal of Engineering Physics and Thermophysics, 87* (2014), 2, pp. 450-458

[34] Volkov, R. S., *et al.*, Evaporation of Two Liquid Droplets Moving Sequentially through High-Temperature Combustion Products, *Thermophysics and Aeromechanics, 21* (2014), 2, pp. 255-258

[35] Kuznetsov, G. V., *et al.*, Motion of Fine-Spray Liquid Droplets in Hot Gas Flow, *Thermophysics and Aeromechanics, 21* (2014), 5, pp. 637-644